Cooperative dipolar relaxation of a glycerol molecular cluster in nanoscale confinement—a computer simulation study

2009 J. Phys.: Condens. Matter 21 425101

(http://iopscience.iop.org/0953-8984/21/42/425101)

IOP Publishing Journal of Physics: Condensed Matter

J. Phys.: Condens. Matter **21** (2009) 425101 (7pp) doi:10.1088/0953-8984/21/42/425101

Cooperative dipolar relaxation of a glycerol molecular cluster in nanoscale confinement—a computer simulation study

Z Dendzik, K Górny and Z Gburski

Institute of Physics, University of Silesia, Uniwersytecka 4, 40-007 Katowice, Poland

Received 22 May 2009, in final form 25 July 2009
Published 8 September 2009
Online at stacks.iop.org/JPhysCM/21/425101

Abstract

We performed an all-atoms molecular dynamics simulation of a glycerol molecular cluster confined in single-walled carbon nanotubes of different diameters to study the confinement size effect on the dipolar relaxation of glycerol molecules. We show that the many-body approach proposed by Dissado and Hill can be directly applied to simulation data and provides quantitative information concerning the cooperative nature of the dipolar relaxation of molecules in nanoscale confinement.

1. Introduction

Properties of molecules in nanoscale confinement are of great interest to biology, geology and materials science [1–3]. Molecular systems embedded in carbon nanotubes [4] are studied not only for fundamental reasons, but also for their potential importance in practical applications in energy storage, nanoelectronic devices, chemical biosensors, field emission displays and many others [5–7]. Glycerol is one of the most extensively studied hydrogen-bonded systems. Because of the presence of three hydroxy groups it has very interesting dynamical and structural properties in condensed phases, it can be easily supercooled reaching the glassy state at about $T_g = 187$ K and its transport coefficients exhibit a non-Arrhenius behavior. Glycerol is also known as one of the best cryoprotectant solvents and has been studied for its capabilities in the long-term preservation of proteins [8, 9].

Dynamics of molecules confined in porous media has been extensively investigated experimentally [10–16] and by means of computer simulations [17–23]. Relaxation of molecular dipoles can be experimentally studied by dielectric relaxation spectroscopy, which proved to be a useful tool to study the dynamics of many molecular systems, such as glass-forming liquids [24, 25], polymers [26], mesophases [27], colloids [28] or ionic conductors [29], over many decades of frequencies. Unlike NMR or vibrational spectroscopy, dielectric relaxation spectroscopy is sensitive to intermolecular interactions and is able to provide information on cooperative processes, providing the link between the methods which probe the properties of the individual molecules and techniques characterizing the bulk properties of the sample [30]. The dielectric relaxation spectrum provides information about individual relaxation processes, their relative amplitudes and characteristic relaxation times of the underlying molecular motions. Although the computer time required to obtain direct information about the relaxation process from all-atoms molecular dynamics simulations is prohibitively large not only in the case of the supercooled state, but also in the case of the deep liquid state, significant progress on glass-forming systems has been obtained from molecular dynamics simulations within computationally accessible limits [31–35], which was related to the development of the mode coupling theory (MCT) [36].

In dynamic measurements, the properties of interest are the material relaxation time and deviation from exponential relaxation. The latter is treated as an outcome of the distribution of the relaxation times or a measure of the cooperativity of the process. The deviation from the exponential relaxation usually follows the stretched exponential or Kohlrausch–Williams–Watts (KWW) [29] characteristic: however, significant deviation from the stretched exponential sometimes occurs for times longer that τ, as reported for glycerol confined in nanoscale pores [10, 37]. Relaxation of molecular systems in confinement is often discussed in terms of the cooperatively rearranging regions and characteristic cooperativity length scale [38]. Because the cooperativity length cannot be larger than the dimensions

of confinement, nanoporous materials are used to study the cooperativity aspects of the glass transition and related dynamics. It is generally agreed that limiting the cooperativity length scale by the confinement leads to accelerated dynamics compared to the bulk: however, the opposite view of the length scale effects has also been proposed [39], suggesting that the cooperativity length represents the amount of material that must be available to enable cooperative reorientation and that nanoscale confinement may lead to decreased mobility. Another issue that has been studied in relation to the concept of the cooperativity length is jamming [40]. The dynamics of the molecules in nanoporous materials is also affected by the interaction with the surface of the pores, which slows down the mobility. Dynamic and thermodynamic measurements reported for the glass transition in confined geometries, for small molecules confined in porous materials as well as for ultrathin polymer films, indicate that T_g decreases, increases or remains the same compared to bulk materials, and that different behaviors have been observed for the same material depending on the experimental method [16]. For confined fragile glass-forming liquids the non-monotonic variation of T_g with decreasing diameter of the pores has also been reported [41]. The access to detailed microscopic information provided by all-atoms molecular dynamics simulations may provide a contribution to our understanding of the process of dynamic formation of cooperatively rearranging regions. In this work, we show that the many-body approach proposed by Dissado and Hill can be directly applied to simulation data, which enables splitting up the observed broadening of the calculated total dipole moment into short- and long-time contributions and provide quantitative information concerning the cooperative nature of the dipolar relaxation of molecules in nanoscale confinement.

2. Simulation details

The glycerol molecule (figure 1) has been modeled by a flexible model based on the CHARMM 27 force field [42], which includes intramolecular harmonic stretching, harmonic bending, torsional, van der Waals and Coulombic terms:

$$V_{\text{total}} = V_{\text{stretch}} + V_{\text{bend}} + V_{\text{torsional}} + V_{\text{vdW}} + V_{\text{Coulomb}}. \quad (1)$$

The intramolecular interactions between the carbon atoms of the nanotube have also been modeled using a flexible model based on the CHARMM 27 force field while the interaction between the nanotube and the glycerol molecule has been modeled using the LJ 12-6 empirical potential, with cutoff 2.0 nm. Parameters of the potential for all interactions in the system have been collected in table 1. The distribution of charge on the glycerol molecule, calculated on B3LYP/6-31***ab initio* data, was taken from [43] and is given in table 2.

The simulated systems consisted of a cluster of glycerol molecules confined inside single-walled open-ended carbon nanotubes of different diameters—(10, 10) nanotube of diameter 13.8 Å, (12, 12) nanotube of diameter 16.6 Å and (15, 15) nanotube of diameter 20.8 Å. The results were then compared to the simulation results of free (unconfined) glycerol molecular clusters. The clusters confined in (10, 10) and (12, 12) nanotubes and for the unconfined cluster consisted of 24 glycerol molecules, whereas the cluster confined inside the (15, 15) nanotube was composed of 32 glycerol molecules. A snapshot of the cluster of glycerol molecules encapsulated in the (10, 10) armchair single-walled carbon nanotube is shown in figure 2. All simulations were performed using the NAMD 2.6 simulation code [44]. The simulations were performed in an NVT ensemble for the temperature $T = 300$ K. Before each trajectory production, the system was equilibrated for 0.2 ns. The classical equations of motion have been integrated using the Brunger–Brooks–Karplus (BBK) method [45] implemented in NAMD 2.6, with the time step of integration of equations of motion being 0.2 fs, which ensures sufficient energy conservation. The steady-state distribution generated by the BBK method has an error proportional to Δt^2 [46], although the error in the time correlation function can have an error proportional to Δt [47]. The temperature was controlled using a Langevin thermostat, with damping coefficient $\gamma = 5.0$ ps^{-1}. All trajectories were produced over 10 000 000 time steps (2 ns). In order to verify to what extent the thermostatting method influences the calculated dipolar relaxation spectra, we continued all runs for the next 10 000 000 time steps in the NVE ensemble, using the velocity Verlet method, and recalculated the autocorrelation functions. We found that the resulting NVE spectra do not differ significantly compared to the NVT results and do not alter the discussion of the results. The results presented in this work were calculated from NVE trajectories.

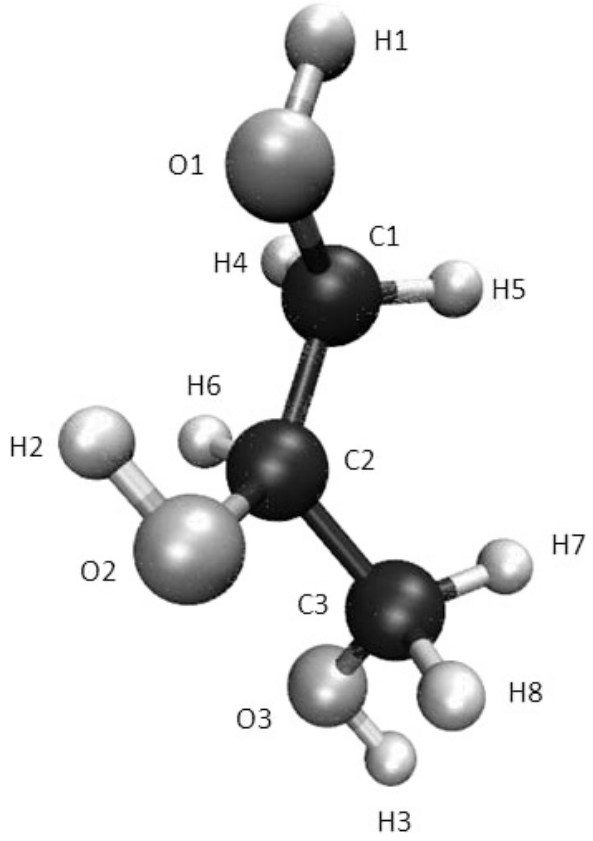

Figure 1. Model of the glycerol molecule.

Table 1. CHARMM force field parameters for glycerol and single-walled carbon nanotube.

$V_{\text{stretch}} = K_r(r - r_0)^2$		
Stretching type	K_r(kcal mol^{-1} A^{-2})	r_0/A
CC	222.500	1.538
CH	309.00	1.111
CO	428.0	1.420
OH	545.0	0.960
CC (SWNT)	305.000	1.3750
$V_{\text{bend}} = K_\Theta(\Theta - \Theta_0)^2$		
Bending type	K_Θ(kcal mol^{-1} rad^{-2})	Θ_0(deg)
CCC	58.350	113.50
CCO	75.700	110.10
CCH	26.500	110.10
COH	57.500	106.00
HCH	35.500	109.00
OCH	45.900	108.89
CCC (SWNT)	40.00	120.00
$V_{\text{torsional}} = \begin{cases} K_\phi(1+\cos(n\phi-\gamma)) & n \neq 0 \\ K_\phi(\phi-\gamma)^2 & n = 0 \end{cases}$		
Torsion type	K_Φ(kcal mol^{-1})	n γ(deg)
CCCH	0.200	3 0.00
CCCO	0.200	3 0.00
OCCO	0.200	3 0.00
OCCH	0.200	3 0.00
HOCC	0.14	3 0.00
HOCH	0.14	3 0.00
HCCH	0.200	3 0.00
CCCC (SWNT)	3.1000	2 180.00
$V_{\text{vdW}} = 4\varepsilon[(\frac{\sigma}{r})^{12} - (\frac{\sigma}{r})^6]$ with Lorentz–Berthelot mixing rules		
Atom type	ε(kcal mol^{-1})	$\sigma/2$ (A)
C (C1, C2)	−0.0560	2.010
C (C2)	−0.0200	2.275
H (H4, H5, H7, H8)	−0.028	1.3400
H (H6)	−0.022	1.3200
H (H1, H2, H3)	−0.046	0.2245
O	−0.1521	1.77
C (SWNT)	−0.070 000	1.992 400

Table 2. Atomic charges on the glycerol molecule. Charges (in electronic units) calculated on B3LYP/6-31**ab initio* data [43].

C1	0.182
C2	0.055
C3	0.182
O1	−0.585
O2	−0.581
O3	−0.585
H1	0.396
H2	0.396
H3	0.396
H4	0.026
H5	0.026
H6	0.040
H7	0.026
H8	0.026

The information about the dipolar relaxation can be obtained from the molecular dynamics trajectories in the

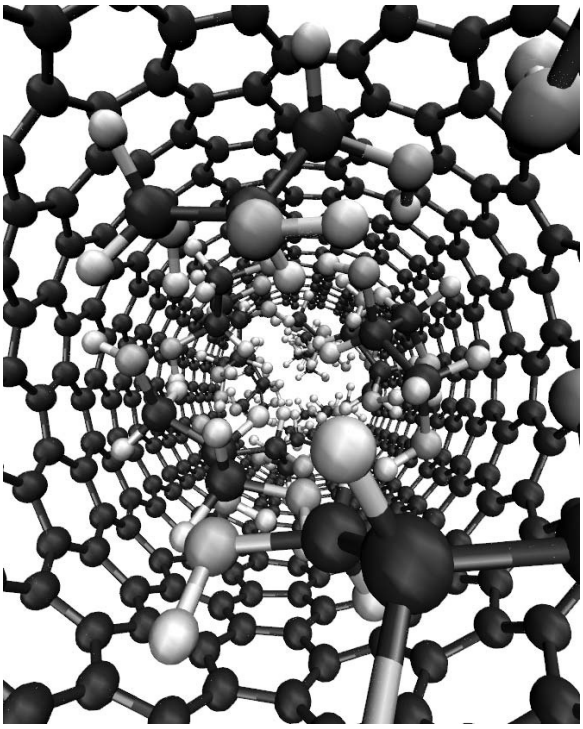

Figure 2. A snapshot of the simulated system—cluster of glycerol molecules encapsulated in (10, 10) armchair single-walled carbon nanotube.

form of the normalized total dipole moment time correlation function (TCF) defined as [48]

$$\Phi(t) = \frac{\langle \vec{M}(0)\vec{M}(t)\rangle}{\langle \vec{M}(0)\vec{M}(0)\rangle}, \tag{2}$$

$$\vec{M}(t) = \sum_{i=1}^{N} \vec{\mu}_i(t) \tag{3}$$

where N is the total number of glycerol molecules and μ_i is the dipole moment of the ith molecule. The connection between the frequency domain dielectric permittivity [29]

$$\varepsilon(\omega) = \varepsilon'(\omega) - i\varepsilon''(\omega), \tag{4}$$

which can be measured in the frequency domain dielectric spectroscopy experiments, and the total dipole moment time correlation function can be introduced as follows:

$$\begin{aligned} \varepsilon'(\omega) &= \varepsilon_0 - (\varepsilon_0 - \varepsilon_\infty)\omega \int_0^\infty \Phi(t)\sin\omega t \,\mathrm{d}t \\ \varepsilon''(\omega) &= (\varepsilon_0 - \varepsilon_\infty)\omega \int_0^\infty \Phi(t)\cos\omega t \,\mathrm{d}, \end{aligned} \tag{5}$$

where $\varepsilon'(\omega)$ is the real part (permittivity factor) and $\varepsilon''(\omega)$ is the imaginary (dielectric loss) part.

In order to verify the usability of our simulation set-up to study dipolar relaxation in glycerol, we produced a test trajectory for bulk glycerol (with periodic boundary conditions and Ewald summation technique) at the temperature T = 350 K and calculated the total dipole moment autocorrelation

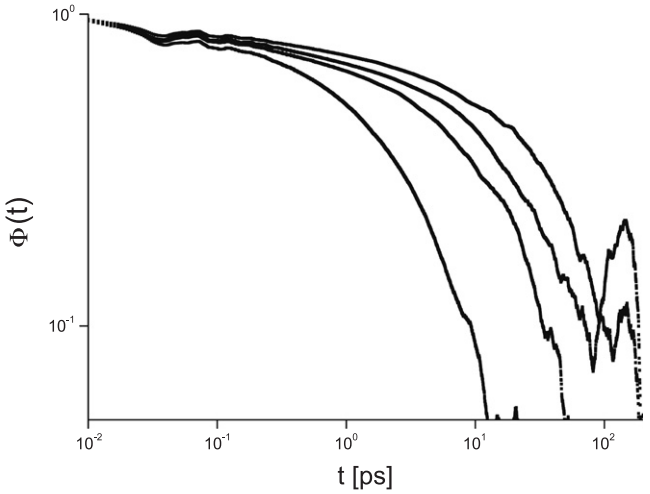

Figure 3. Master plot of the total dipole moment autocorrelation functions calculated for unconfined cluster of glycerol molecules and for the clusters confined in (15, 15), (12, 12) and (10, 10) nanotubes (from left to right, respectively).

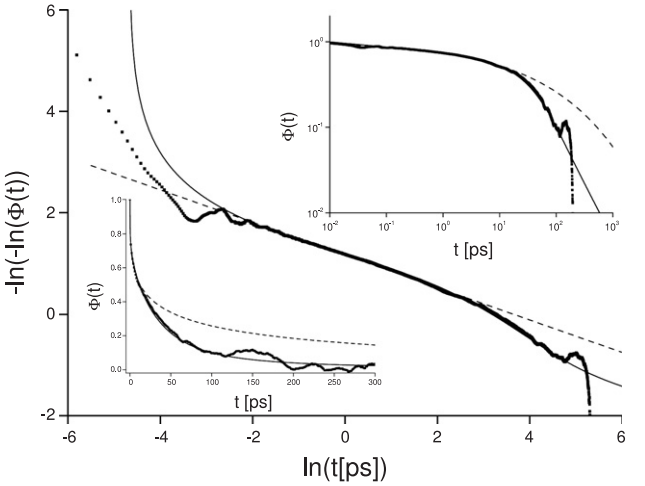

Figure 4. Calculated total dipole moment autocorrelation function of glycerol molecules confined in (10, 10) single-walled carbon nanotube in the coordinates which enable us to assess the KWW fit (dashed line). Solid line represents the DH fit to the data. The insets show the same in the usual log–linear and log–log representations.

function and frequency dipole relaxation spectrum in order to compare the resulting spectra with available broadband dielectric spectroscopy experimental data [25]. The calculated values of the loss peak frequency $f_{\max} = 1.4$ GHz and the loss high-frequency slope $n = 0.56$ agree satisfactorily with the experimental values of $f_{\max} = 1.6$ GHz and $n = 0.60$ estimated from the dielectric spectroscopy results [25].

3. Results and discussion

We studied the dipolar relaxation of the glycerol molecules confined in open-ended single-walled carbon nanotubes of different diameters. As a reference system, we have also simulated the relaxation process in a free glycerol molecular cluster. Figure 3 shows the time correlation function of the normalized total dipole moment for all studied systems, showing that the relaxation rate of the glycerol cluster essentially decreases with the size of nanotube confinement. Aside from the relaxation rate, the nanotube confinement considerably influences also the shape of the relaxation spectra. In order to infer more quantitative information from the change of shape of the calculated spectra, we fitted the data with the KWW decay function:

$$\Phi(t) = \exp(-(t/\tau_{\mathrm{KWW}})^{\beta}), \tag{6}$$

where τ_{KWW} is the characteristic relaxation time and $0 < \beta < 1$ is the parameter measuring the broadening of the relaxation spectrum. The latter is often treated as a measure of the distribution of the relaxation times or as a measure of the cooperativity of the relaxation process [29]. As the KWW fit turned out to be satisfactory only in the case of the unconfined glycerol cluster and was not appropriate in the case of confined systems, we refitted the data with the relaxation function developed from the many-body approach proposed by Dissado and Hill (DH) [49]:

$$\Phi(t) = \frac{\Gamma(1+m-n)}{\Gamma(2-n)\Gamma(1+m)}\frac{1}{\tau_{\mathrm{DH}}} \times A\mathrm{e}^{-t/\tau_{\mathrm{DH}}}(t/\tau_{\mathrm{DH}})^{-n}{}_1F_1(1-m;2-n;t/\tau_{\mathrm{DH}}), \tag{7}$$

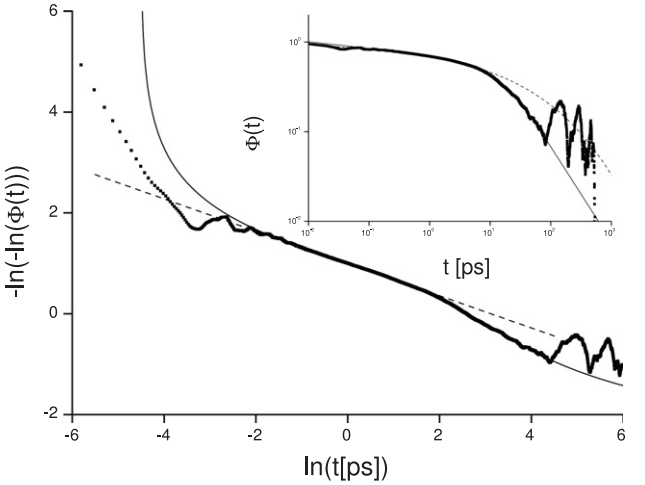

Figure 5. Calculated total dipole moment autocorrelation function of glycerol molecules confined in (12, 12) single-walled carbon nanotube. Solid and dashed lines are DH and KWW fits, respectively. The inset shows the same in the log–log representation.

where τ_{DH} is the characteristic relaxation time, Γ is the Euler gamma function, ${}_1F_1$ denotes the Kummer confluent hypergeometric function [49] and A is a normalizing constant. The DH function has two parameters n and m describing the shape of the spectrum in the short-time regime and long-time regime, instead of a single parameter β for the KWW expression describing the broadening of the spectrum over the whole time regime.

Figures 4–6 show the total moment autocorrelation functions calculated for the glycerol molecular cluster confined in nanotubes of different diameters in coordinates which enable us to assess the KWW fit to the data. The insets show the same in the usual log–log representation. Figure 7 shows the reference data calculated for free (unconfined) glycerol clusters. In all cases, the solid lines are DH and the

Table 3. KWW and DH fitting parameters for the total dipole moment autocorrelation function of glycerol confined in carbon nanotubes and for unconfined cluster of glycerol molecules ($T = 300$ K).

	τ_{KWW}/ps	β	τ_{DH}/ps	n	m
Cluster confined in (10, 10) nanotube	38.71	0.320	26.84	0.061	0.265
Cluster confined in (12, 12) nanotube	22.18	0.322	13.36	0.073	0.052
Cluster confined in (15, 15) nanotube	11.93	0.346	7.78	0.077	0.084
Free (unconfined) cluster	2.01	0.544	2.06	0.087	0.228

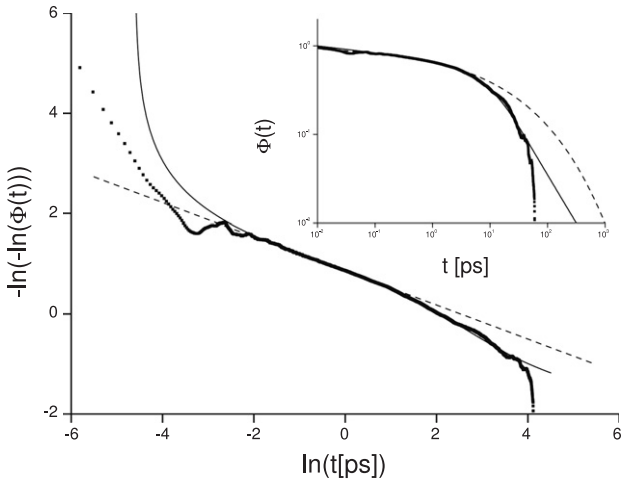

Figure 6. Calculated total dipole moment autocorrelation function of glycerol molecules confined in (15, 15) single-walled carbon nanotube. Solid and dashed lines are DH and KWW fits, respectively. The inset shows the same in the log–log representation.

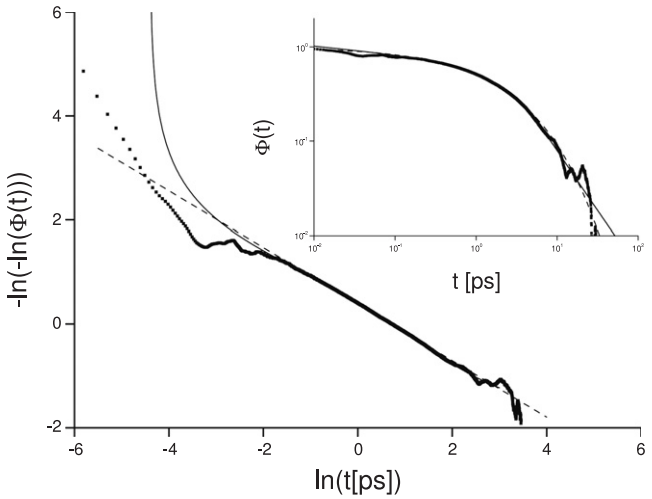

Figure 7. Calculated total dipole moment autocorrelation function of free (unconfined) cluster of glycerol. Solid and dashed lines are DH and KWW fits, respectively. The inset shows the same in the log–log representation.

dashed lines are KWW fits to the calculated data. In the case of the unconfined cluster (figure 7), the dipole moment autocorrelation function can be represented reasonably well by a single KWW stretched exponential in the whole time regime. In the case of the confined clusters, the dipole moment autocorrelation function can be described by a single KWW function approximately up to the time corresponding to the characteristic relaxation time of the system and cannot be described for longer times, where significant deviation from the single stretched exponential behavior occurs. The values of the characteristic relaxation time calculated from the KWW and DH fits are collected in table 3 along with the values of β, n and m.

A few regions can be distinguished in the relaxation spectra, as they are shown in figures 4–7. For the shortest times, which correspond to the far-infrared range of the spectrum, the relaxation clearly does not follow the KWW stretched exponential. Instead, it follows a Gaussian law $\exp(-at^2)$ terminated by a period of oscillatory behavior. This feature agrees well with the theoretical predictions of Dissado and Hill (DH) [50, 29]. For longer times, the relaxation can be well reproduced by the KWW stretched exponential function. Its asymptotic behavior can be related to the shape parameter n. DH theory provides the meaning of this parameter as a measure of the so-called intra-cluster cooperativity of the relaxation, where a cluster is defined as a subassembly of molecules relaxing coherently with n being a measure of the degree of this coherence. According to DH theory, this region ends approximately at a time corresponding to the relaxation time of the system, at which the relaxation of subassemblies is annihilated through exchange energy with the phonon bath. The solution of the relaxation equation in this narrow region is the exponential $\exp(-t/\tau)$ known as Debye relaxation. For longer times, the relaxation evolves into its final stage, which can be identified in the case of the confined clusters (figures 4–6), and which is characterized by the deviation from the single KWW stretched exponential behavior. Dissado and Hill [50, 29] attributes the asymptotic behavior of the relaxation, measured by the shape parameter m, with the so-called inter-cluster relaxation, related to exchanging the relaxing molecules between the more or less cooperatively rearranging regions. The deviation from the single KWW behavior for the times $t > \tau$ (figures 4–6) corresponds to the DH characteristic and suggests that the presence of the nanotube confinement affects the formation of cooperatively rearranging regions and influences the degree of coherence between them.

Although, apart from the asymptotic behavior at low- and high-frequency regimes, the exact shape of the DH susceptibility function (Fourier transform of the solution of the DH relaxation equation) [50] is difficult to verify experimentally, some work suggested that the DH susceptibility function is more appropriate to describe the dielectric spectroscopy data than other routinely used fitting functions [51, 52] and may rationalize the scaling behavior

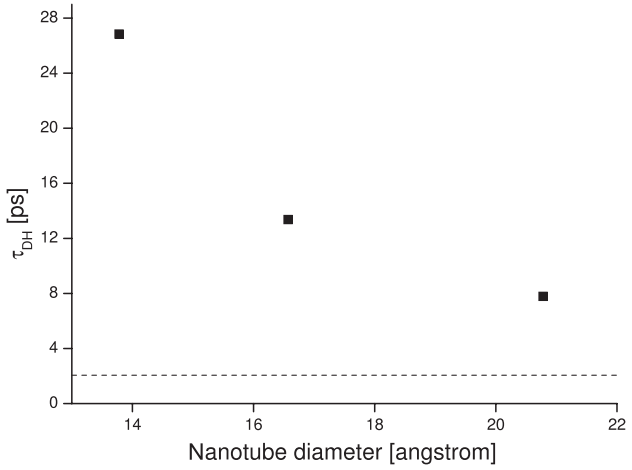

Figure 8. Effect of the nanosize confinement on the characteristic relaxation rate τ_{DH} of the DH function. The points represent τ_{DH} values calculated for the systems encapsulated in (10, 10), (12, 12) and (15, 15) nanotubes (from left to right, respectively). Dashed line denotes the value for an unconfined cluster.

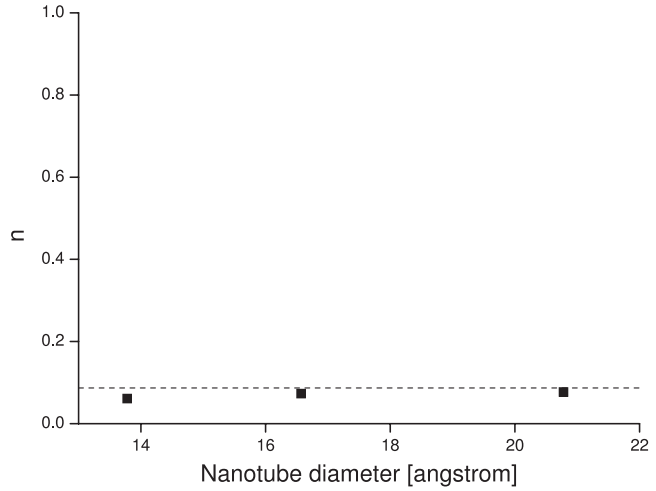

Figure 9. Effect of the nanosize confinement on the short-range correlation parameter n of the DH function.

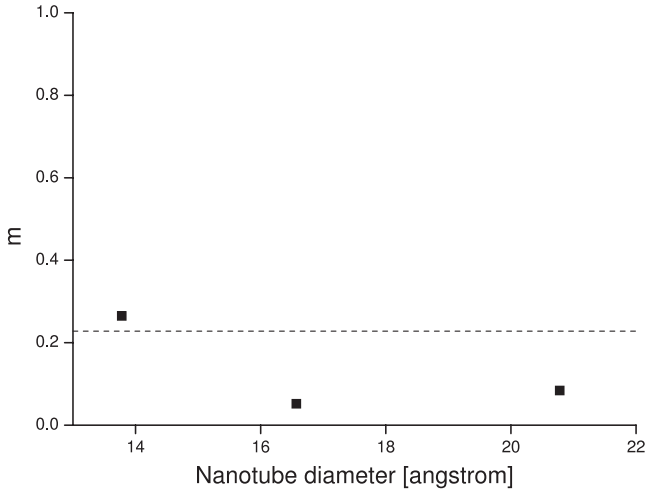

Figure 10. Effect of the nanosize confinement on the long-range correlation parameter m of the DH function.

observed in the dielectric response of many systems [53, 54]. The deviation from the single KWW stretched exponential behavior in the case of glycerol molecules confined in nanotubes provides the rationale for the dielectric spectroscopy results of Pissis *et al* [10] who studied dielectric relaxation of liquid glycerol, propylene glycol and propylene carbonate confined in Vycor glass (with porosity 0.28, internal surface area 250 $m^2\ g^{-1}$ and an average pore diameter of 4 nm) and reported that, in contrast to bulk liquids, their spectra for confined liquids could not be fitted with the KWW-type fitting form, which supports the conclusion that the confinement not only shifts the relaxation time and affects the β parameter of the KWW fit, but also imposes more essential changes on the relaxation mechanism.

The dependence of the size of the nanotube confinement on the relaxation time τ_{DH} and the cooperativity parameters n and m is illustrated in figures 8–10. The first conclusion is that the relaxation of the free cluster of glycerol molecules simulated at the temperature $T = 300$ K is faster by three orders of magnitude than the relaxation of the bulk glycerol liquid measured experimentally at the temperature $T = 300$ K [25] and faster by almost two orders than the relaxation time in simulated bulk glycerol at $T = 350$ K (this work). The relaxation time for the free cluster is $\tau_{DH} = 2.06$ ps. The nanotube confinement shifts the relaxation time from $\tau_{DH} = 7.78$ ps in the case of the (15, 15) nanotube to $\tau_{DH} = 26.84$ ps in the case of the (10, 10) nanotube, which was the narrowest nanotube considered in this study. The value of the short-time parameter n for the free cluster is $n = 0.087$. Confining the free cluster inside a nanotube only slightly affects the value of the parameter n, from $n = 0.077$ in the case of the (15, 15) nanotube, up to $n = 0.061$ in the case of the narrowest (10, 10) nanotube. On the other hand, the confinement strongly affects the value of the parameter m, which varies from $m = 0.084$ in the case of a cluster embedded in the (15, 15) nanotube, to $m = 0.265$ in the case of the cluster embedded in the (10, 10) nanotube. The value for the unconfined cluster is $m = 0.228$. Moderate and systematic changes of the parameter n indicate that the presence of confinement does not considerably affect the correlation between individual dipoles. On the other hand, significant changes of the parameter m suggest that the confinement considerably affects the dynamic formation of cooperatively rearranging regions in the studied system. The nonsystematic change in the value of parameter m with nanotube diameter can be understood in terms of the different geometry (aspect ratio) imposed by the nanotube of different diameters on the studied glycerol system. The above conclusions cannot be inferred from the usual analysis of the change in the parameter β of the KWW fit, as it appropriately describes only the short-time portion of the relaxation spectrum and is insensitive to the change in the portion of the spectrum related to the correlations between the cooperatively rearranging regions.

4. Conclusions

The characteristic of the dipolar relaxation process in nanoscale confinement is an outcome of a counterbalance between interaction between the host and guest systems and the change of the length scale of the cooperatively rearranging regions imposed by the geometrical constraints. Embedding the glycerol molecular cluster into a nanotube considerably shifts the relaxation time towards longer times and broadens significantly the shape of the total dipole moment autocorrelation function, which suggests a more cooperative relaxation. The dipole moment autocorrelation function follow the KWW stretched exponential characteristic only in the case of an unconfined cluster of glycerol molecules. In the case of the molecules confined in nanotubes, considerable deviation from stretched exponential behavior occurs, which agrees well with reported results of dielectric spectroscopy results for glycerol in porous glasses. This deviation from stretched exponential can be described and rationalized in the framework of the many-body theory proposed by Dissado and Hill. This approach allows us to split up the observed broadening of the calculated spectra into a short-time contribution related to correlations between movements of individual dipoles and a long-time contribution reflecting the correlations between cooperatively rearranging regions. All-atoms molecular dynamics simulations of nanoconfined glass-forming liquids in the computationally accessible temperature regime may contribute to understanding the process of dynamic formation of cooperatively rearranging regions and to examine the characteristic cooperativity length scale.

References

[1] Morishige K and Kawano K 1999 *J. Chem. Phys.* **110** 4867
[2] Mitra S, Mukhopadhyay R, Tsukushi I and Ikeda S 2001 *J. Phys.: Condens. Matter* **13** 8455
[3] Raviv U, Laurat P and Klein J 2001 *Nature* **413** 51
[4] Kolesnikov A, Zanotti J, Loong C, Thiyagarajan P, Moravsky A, Loutfy R and Burnham C 2004 *Phys. Rev. Lett.* **93** 35503
[5] Dillon A, Jones K, Bekkedahl T, Kiang C, Bethune D and Heben M 1997 *Nature* **386** 377
[6] Chen P, Wu X, Lin J and Tan K 1999 *Science* **285** 91
[7] Lu J and Han J 1998 *Int. J. High Speed Electron. Syst.* **9** 101
[8] Cicerone M and Soles C 2004 *Biophys. J.* **86** 3836
[9] Caliskan G, Mechtani D, Roh J, Kisliuk A, Sokolov A, Azzam S, Cicerone M, Lin-Gibson S and Peral I 2004 *J. Chem. Phys.* **121** 1978
[10] Pissis P, Daoukaki-Diamanti D, Apekis L and Christodoulides C 1994 *J. Phys.: Condens. Matter* **6** L325
[11] Wendt H and Richert R 1999 *J. Phys.: Condens. Matter* **11** A199
[12] Gorbatschow W, Arndt M, Stannarius R and Kremer F 1996 *Europhys. Lett.* **35** 719
[13] Streck C, Mel'nichenko Y B and Richert R 1996 *Phys. Rev.* B **53** 5341
[14] Liu G, Mackowiak M, Li Y and Jonas J 1991 *J. Chem. Phys.* **94** 239
[15] Bergman R, Mattsson J, Svanberg C, Schwartz G A and Swenson J 2003 *Eur. Phys. Lett.* **64** 675
[16] Alcoutlabi M and Mckenna G B 2005 *J. Phys.: Condens. Matter* **17** R461
[17] Scheidler P, Kob W and Binder K 2000 *Europhys. Lett.* **52** 277
[18] Scheidler P, Kob W and Binder K 2002 *Europhys. Lett.* **59** 701
[19] Brovchenko I, Geiger A, Oleinikova A and Paschek D 2003 *Eur. Phys. J.* E **12** 69
[20] Rovere M and Gallo P 2003 *Eur. Phys. J.* E **12** 77
[21] Marti J and Gordillo M C 2002 *J. Chem. Phys.* **114** 10486
[22] Marti J and Gordillo M C 2003 *J. Chem. Phys.* **119** 12540
[23] Dawid A and Gburski Z 2007 *J. Non-Cryst. Solids* **353** 4339
[24] Das S 2004 *Rev. Mod. Phys.* **76** 785
[25] Hofmann A, Kremer F, Fischer E and Schonhals A 1994 *Disorder Effects on Relaxation Processes* ed R Richert and A Blumen (Berlin: Springer)
[26] Ku C and Liepins R 1987 *Electrical Properties of Polymers* (Muenchen: Hanser)
[27] Blinov L 1983 *Electro-Optical and Magneto-Optical Properties of Liquid Crystals* (Chichester: Wiley)
[28] Feldman Y 2001 *Dielectric Spectroscopy on Colloidal Systems-a Review* (*Encyclopedia Handbook of Emulsion Technology* vol 5) ed P Becher (New York: Dekker)
[29] Jonscher A 1983 *Dielectric Relaxation in Solids* (London: Chelsea Dielectric)
[30] Paluch M, Dendzik Z and Rzoska S 1999 *Phys. Rev.* B **60** 2979
[31] Kob W and Andersen H 1995 *Phys. Rev.* E **52** 4134
[32] Mossa S, Ruocco G and Sampoli M 2001 *Phys. Rev.* E **64** 021511
[33] Sastry S 2001 *Nature* **409** 164
[34] Bordat P, Lerbret A, Affouard F, Demaret J and Descamps M 2004 *Europhys. Lett.* **65** 41
[35] Chong S and Sciortino F 2004 *Phys. Rev.* E **69** 51202
[36] Gotze W, Hansen J, Levesque D and Zinn-Justin J 1990 *Liquids Freezing and the Glass Transition* (New York: North-Holland)
[37] Dendzik Z, Gorny K, Kosmider M and Zurek S 2009 *J. Opt. Adv. Mater.* at press
[38] Adam G and Gibbs J H 1965 *J. Chem. Phys.* **43** 139
[39] Mckenna G B 2003 *Eur. Phys. J.* E **12** 191
[40] Torquato S 2002 *Random Heterogeneous Materials Microstructure and Macroscopic Properties* (New York: Springer)
[41] Alba-Simionesco C, Dosseh G, Dumont E, Frick B, Geil B, Morineau D, Teboul V and Xia Y 2003 *Eur. Phys. J.* E **12** 19
[42] MacKerell A D Jr, Feig M and Brooks C III 2004 *J. Comput. Chem.* **25** 1400 and references therein
Feller S and MacKerell A D Jr 2000 *J. Phys. Chem.* B **104** 7510
[43] Chelli R, Procacci P, Cardini G, Valle R and Califano S 1999 *Phys. Chem. Chem. Phys.* **1** 871
[44] Phillips J, Braun R, Wang W, Gumbart J, Tajkhorshid E, Villa E, Chipot C, Skeel R, Kale L and Schulten K 2005 *J. Comput. Chem.* **26** 1781
[45] Brunger A, Brooks C L and Karplus M 1984 *Chem. Phys. Lett.* **105** 495
[46] Mishra B and Schlick T 1996 *J. Chem. Phys.* **105** 299
[47] Wang W and Skeel R D 2003 *Mol. Phys.* **101** 2149
[48] Guardia E and Marti J 2004 *Phys. Rev.* E **69** 011502
[49] Abramovitz M and Stegun I 1972 *Handbook of Mathematical Functions* (New York: Dover)
[50] Dissado L A and Hill R M 1983 *Proc. R. Soc.* A **390** 131
[51] Forsman H 1989 *J. Phys. D: Appl. Phys.* **22** 1528
[52] Dendzik Z and Gburski Z 1997 *J. Mol. Struct.* **410** 237
[53] Dendzik Z, Paluch M, Gburski Z and Ziolo J 1997 *J. Phys.: Condens. Matter* **9** L339
[54] Schneider U, Brand R, Lunkenheimer P and Loidl A 2000 *Eur. Phys. J.* E **2** 67